

PACS 72.20.J, 78.60.J

The influence of the exciton non-radiative recombination in silicon on the photoconversion efficiency.

1. Long Shockley–Read–Hall lifetimes

A.V. Sachenko^{1,*}, V.P. Kostilyov¹, V.M. Vlasiuk¹, I.O. Sokolovskiy¹, M.A. Evstigneev²

¹*V. Lashkaryov Institute of Semiconductor Physics, NAS of Ukraine,
41, prospect Nauky, 03028 Kyiv, Ukraine*

²*Department of Physics and Physical Oceanography,*

Memorial University of Newfoundland, St. John's, NL, A1B 3X7 Canada

**E-mail: sach@isp.kiev.ua*

Abstract. By comparison of the experimental dependence of bulk lifetime in silicon on the doping and excitation levels with theoretical calculations, it has been shown that a new recombination channel becomes operative when Shockley–Read–Hall lifetime is below 20 ms and the density of doping impurities or the excess electron-hole pair density is of the order of 10^{16} cm^{-3} . This recombination mechanism is related to the non-radiative exciton Auger recombination assisted by the deep impurities in the bulk. The influence of non-radiative exciton recombination on the photoconversion efficiency in solar cells has been analyzed. It has been shown that the shorter the Shockley–Read–Hall lifetime, τ_{SHR} , the stronger its effect. In particular, for $\tau_{\text{SHR}} = 100 \mu\text{s}$, this recombination channel leads to the reduction of the photoconversion efficiency by 5.5%.

Keywords: solar cells, photoconversion, non-radiative exciton recombination, Shockley–Read–Hall lifetime.

Manuscript received 01.07.16; revised version received 22.09.16; accepted for publication 16.11.16; published online 05.12.16.

1. Introduction

In the recent few decades, the photoconversion efficiency of silicon structures, such as *p-n* junction- and heterojunction-based solar cells (SCs), has been boosted to the value of 25% [1-3]. It was achieved using high-quality silicon with the non-equilibrium electron-hole pair lifetimes of the order of a few milliseconds at low doping levels, as well as by employing various passivation methods to obtain very low surface recombinations velocities [4, 5]. To further increase the photoconversion efficiency, it is necessary to optimize

several parameters of the base region, in particular, the doping level and thickness. As pointed out in [4], at such long bulk lifetimes, even at not very high doping and excitation levels, n_0 and Δn , respectively, radiative and band-to-band Auger recombination processes become operative, which limits the effective bulk lifetime and the output power of SC.

The questions related to the influence of radiative and Auger recombination in silicon on the effective lifetime have been discussed extensively in the literature, see [5] and references therein. In spite of the fact that a good agreement between theoretical and experimental

findings has been achieved for doping and excitation levels exceeding 10^{16} cm^{-3} , the region below 10^{16} cm^{-3} seems to be understood to a lesser degree (here). In particular, Fossum [6], being based on the experimental data from [7, 8], proposed the following empirical expression for the reduction of the effective lifetime in silicon with doping level:

$$\tau_{eff}(n) = \frac{\tau_{max}}{1 + (n/n_x)}, \quad (1)$$

where the electron-hole pair density, $n = n_0 + \Delta n$, is the sum of the equilibrium, n_0 , and the excess, Δn , contributions, and $n_x = 7.1 \cdot 10^{15} \text{ cm}^{-3}$ both for p - and n -type semiconductors.

As seen from (1), the decrease of τ_{eff} begins at the doping levels of the order of 10^{16} cm^{-3} , *i.e.* well before the band-to-band Auger recombination starts to take place.

Finally, the PC1D code uses an empirical expression $\tau_{eff} \propto (n/n_x)^{-\alpha}$, which takes into account, according to the code developers, the influence of crystal growth on the effective lifetime in silicon. When the first version of this code was released a few decades ago, there apparently were reasons to relate the decrease of τ_{eff} with n to the technological factors at low doping, although the fact that n_x is practically the same for n - and p -type semiconductors remained unexplained. However, as far as more modern works are concerned, such as [5], this explanation cannot be applied in view of the absence of such uncontrolled technological factors, which was possible to achieve in recent years.

As will be shown below, the region described by the empirical formula (1) is realized in the experimental $\tau_{eff}(n)$ curves from [4, 7-9], although it is absent in the analogous data from [5]. Its presence or absence is determined by the Shockley–Read–Hall lifetime: if $\tau_{SRH} \geq 20 \text{ ms}$, radiative recombinations dominates over the quadratic non-radiative one, and the decrease of $\tau_{eff}(n)$ according to $\tau_{SRH}(n)n_x/n$ is absent. In the opposite case, quadratic non-radiative recombination takes over, leading to the onset of a region described by (1). We relate this region to the non-radiative impurity-assisted Auger recombination of the excitons generated in silicon by light. In this work, the influence of this recombination channel on the photoconversion efficiency of heterojunction SCs is analyzed, and the SC design is optimized with respect to the base doping level. It is shown that the lower τ_{SRH} , the stronger the efficiency reduction due to the non-radiative exciton recombination.

2. Analysis of the literature data on τ_{eff}

In our analysis of the effective lifetime reported in the literature, especially in [5], we employ the following expression for the main quantity of interest, the effective lifetime:

$$\tau_{eff}(n) = \left[\frac{1}{\tau_{SRH}(n)} + \frac{1}{\tau_r(n)} + \frac{1}{\tau_{nr}(n)} + \frac{1}{\tau_{Auger}(n)} \right]^{-1}, \quad (2)$$

where τ_r , τ_{nr} , and τ_{Auger} are the radiative, non-radiative, and Auger lifetimes, respectively, with

$$\tau_{nr} = \tau_{SRH} \frac{n_x}{n}, \quad (3)$$

and the Shockley–Read–Hall lifetime in n -type silicon is given by

$$\tau_{SRH}^n(n) \cong \frac{\tau_{p0}(n_0 + n_1 + \Delta n) + \tau_{n0}(p_1 + \Delta n)}{n_0 + \Delta n}, \quad (4)$$

where $\tau_{p0} = (C_p N_t)^{-1}$, $\tau_{n0} = (C_n N_t)^{-1}$, $C_{p,n}$ are the coefficients of hole and electron capture by recombination centers (traps) of the density N_t , and n_1 and p_1 are the electron and hole densities in the case when the recombination level coincides with the Fermi energy.

Radiative lifetime is given by the expression

$$\tau_r^{-1} = A(n_0 + \Delta n), \quad (5)$$

where the radiative recombination parameter obtained in [10], taking into account both band-to-band and exciton radiative recombination, varies at room temperature from $A = 6.3 \cdot 10^{-15} \text{ cm}^3/\text{s}$ at $n = 10^{15} \text{ cm}^{-3}$ to $4.63 \cdot 10^{-15} \text{ cm}^3/\text{s}$ at $n = 10^{16} \text{ cm}^{-3}$. For numerical estimates, we will use the value $A = 6.3 \cdot 10^{-15} \text{ cm}^3/\text{s}$, because at $n = 10^{16} \text{ cm}^{-3}$ the band-to-band Auger recombination dominates in silicon, so that the inaccuracy in A will practically not affect the calculation results.

As for the band-to-band lifetime $\tau_{Auger}(n)$, we used the empirical expression given by Eq. (18) in [5].

Before analyzing $\tau_{eff}(n)$, we note that, depending on the energy of the recombination center and electron and hole capture cross section, the Shockley–Read–Hall lifetime as a function of the electron-hole pair density varies between two values and may increase, decrease, or remain practically the same in a certain range of doping and excitation levels. In what follows, we will mainly consider the case where τ_{SRH} is practically constant in the range of interest, where the doping level changes from 10^{14} to 10^{17} cm^{-3} , and the excitation level from 10^{14} to 10^{16} cm^{-3} .

Presented in Figs. 1a and 1b are the experimental $\tau_{eff}(n)$ curves for n - and p -type semiconductors, respectively. The experimental data points are taken from [5, 7, 11, 12], and the theoretical curves are plotted using (2)-(5), as well as the expressions (18) and (19) for τ_{Auger} from Ref. [5]. There are two fit parameters in the theory: the density of the deep levels, which defines τ_{SRH} and n_x . In principle, they can be found separately by measuring $\tau_{eff}(n)$ at the doping levels below 10^{14} cm^{-3} .

As seen in Fig. 1a, the theoretical curves agree well with the experimental results from [7] at $n_x = 8.2 \cdot 10^{15} \text{ cm}^{-3}$, found using the least squares method. As for p -type semiconductor, Fig. 1b, the theoretical curves plotted with and without taking the additional quadratic recombination channel into account do not differ much from each other.

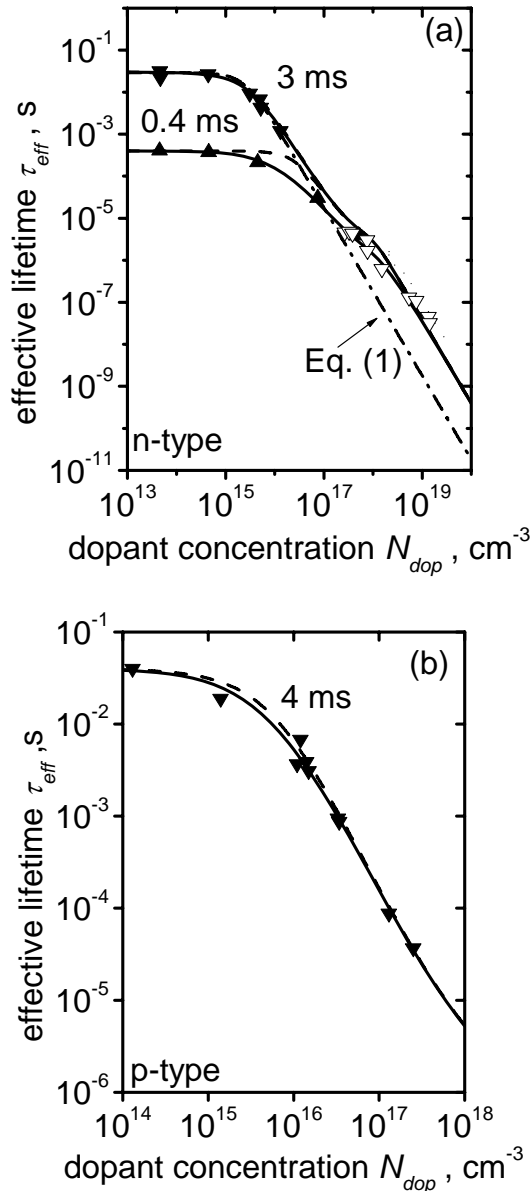


Fig. 1. Effective lifetime in (a) n - and (b) p -type silicon vs. the doping level. Solid lines are obtained with and dashed lines without taking the exciton recombination effect into account. Symbols: experimental results from [5] (down filled triangles), [6] and [7] (up filled triangles), [12] (up open triangles), [11] (down open triangles). The theoretical curves were plotted with $n_x = 8.2 \cdot 10^{15} \text{ cm}^{-3}$ for (a) $\tau_{\text{SRH}} = 3 \text{ ms}$ (red) and $\tau_{\text{SRH}} = 0.4 \text{ ms}$ (blue), and (b) $\tau_{\text{SRH}} = 4 \text{ ms}$. Note that for $\tau_{\text{SRH}} = 3 \text{ ms}$, the curves obtained with and without exciton recombination effect practically coincide. The dotted curve was obtained from Eq. (1).

Fig. 2 shows the experimental results for $\tau_{\text{Auger}}(n)$ in n - and p -type silicon from [9]. The theoretical curves $\tau_{\text{eff}}(n)$ were obtained from the reduced version of (2), where the term τ_r was omitted, and Eqs. (18) and (19) from [9]. As seen in Fig. 2a, including the additional recombination channel has a practical effect on the theoretical curves for n -type silicon. At the same time, for p -type semiconductor, the theoretical curves agree with the experimental ones only when it is taken into account with $n_x = 8.2 \cdot 10^{15} \text{ cm}^{-3}$.

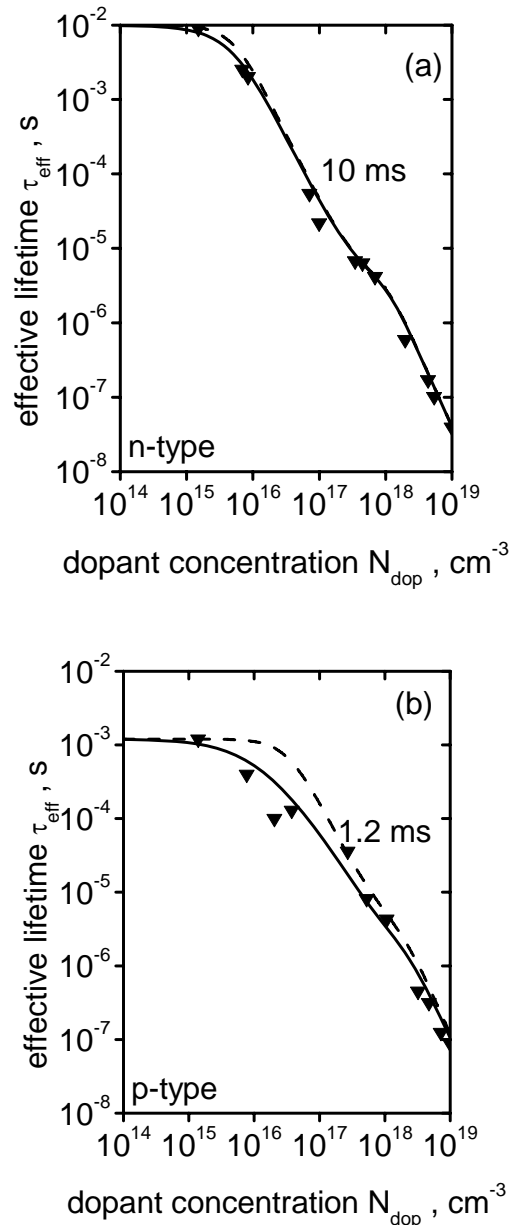


Fig. 2. Reduced effective bulk lifetime τ_{eff}^* vs. the doping level in (a) n - and (b) p -type silicon. The theoretical curves were obtained for (a) $\tau_{\text{SRH}} = 10 \text{ ms}$ and (b) $\tau_{\text{SRH}} = 1.2 \text{ ms}$ with (solid lines) and without (dashed ones) taking exciton recombination into account. Down triangles: experimental data from [9].

Shown in Fig. 3 is the effective lifetime vs. the excitation level, where the experimental data points are taken from [4, 5], and the theoretical ones were obtained from (2)-(5) and the expressions (18) and (19) from [5]. In the case of *n*-type semiconductor (Fig. 3a), the theory with $n_x = 8.2 \cdot 10^{15} \text{ cm}^{-3}$ agree well with the experiment, although the theoretical curves $\tau_{eff}(n)$ for the sample with the orientation $\langle 111 \rangle$ are practically the same with and without exciton non-radiative recombination channel. On the other hand, in the *p*-type case, Fig. 3b, the theory cannot fit the experimental data, unless the dependence $\tau_{SRH}(n)$ is taken into account. To achieve agreement, we assumed that for *p*-type silicon, the levels are operative, if their energy is 0.38 eV, and that $\tau_{p0} = 3.6 \cdot 10^{-2} \text{ s}$, $\tau_{n0} = 2.4 \cdot 10^{-1} \text{ s}$.

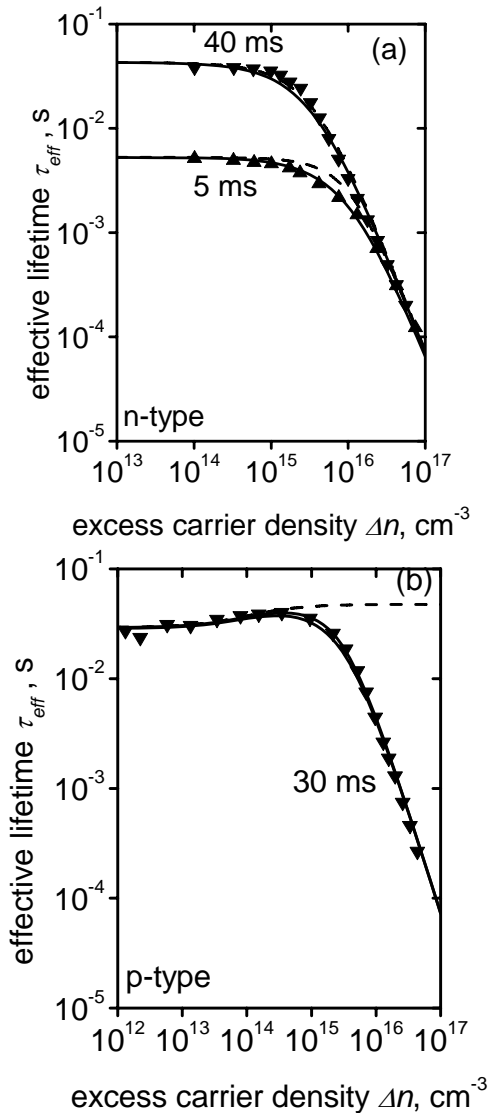


Fig. 3. Effective bulk lifetime vs. the excess electron-hole pair density for (a) *n*- and (b) *p*-type silicon. The theoretical curves were obtained with (solid lines) and without (dashed lines) taking exciton recombination into account. The dash-dotted curve describes $\tau_{SRH}(n)$ for the cobalt level $n_x = 8.2 \cdot 10^{15} \text{ cm}^{-3}$. Experimental points in the panel (a) are taken from Ref. [4] for $\langle 111 \rangle$ (down triangles) and $\langle 100 \rangle$ (up triangles) orientation, and in (b) from Ref. [5] (squares).

In order to find out the conditions, under which the additional quadratic recombination channel has a noticeable effect on τ_{eff} , we need to compare it to the radiative recombination channel's contribution. When these two recombination channels are of equal importance, we have the relation $A = (\tau_{SRH}^* n_x)^{-1}$, from which we can determine that value of Shockley–Read–Hall, τ_{SRH}^* , at which the radiative recombination starts to dominate. For $n_x = 8.2 \cdot 10^{15} \text{ cm}^{-3}$, this gives $\tau_{SRH}^* \approx 20 \text{ ms}$. For $\tau_{SRH} > 20 \text{ ms}$, radiative recombination dominates, whereas for $\tau_{SRH} < 20 \text{ ms}$, non-radiative recombination is more important. As seen from Figs. 1 to 3, this criterion is applicable to all the cases considered. Because the Shockley–Read–Hall lifetime in today's high-efficiency *p-n*- or heterojunction-based SCs is of the order of a few milliseconds, quadratic non-radiative recombination channel must be taken into account during the analysis of photoconversion efficiency.

Also, Figs. 1 to 3 indicate that, at τ_{SRH} lower than 1 ms, the role of quadratic non-radiative recombination becomes essential. This is seen, in particular, in Fig. 1a for $\tau_{SRH} = 0.4 \text{ ms}$, which exhibits quite a broad region that cannot be described by (1) with radiative and band-to-band Auger recombination channels only. Therefore, we need to find the physical explanation of the experimental $\tau_{eff}(n)$ curves described by (1). This explanation was proposed in [13], which is briefly reviewed here.

3. Non-radiated exciton recombination in silicon

Sufficiently strong irradiation of silicon generates not only electron-hole pairs of density Δn but also excitons of density n_{exc} . Although $n_{exc} \ll \Delta n$, the exciton non-radiative lifetime τ_{nr} , related to their Auger recombination assisted by deep impurity levels can in many cases be much shorter than the Shockley–Read–Hall lifetime τ_{SRH} . This leads to binding of excess electron-hole pairs into excitons, which then recombine [13, 14]. This process was first considered by Hangleiter [14], who showed that both Auger and Shockley–Read–Hall recombination can be mediated by the same deep level.

In the work [13], a phenomenological relation between τ_{nr} and τ_{SRH} was proposed being based on the following two premises. First, it was assumed that the non-equilibrium electron-hole pair density, n , and exciton density, n_{exc} , are related by

$$n_{exc} = \frac{(n_0 + \Delta n)\Delta n}{n^*}, \quad n^* = \frac{N_c N_v}{N_x'} e^{-E_x/kT}, \quad (6)$$

where N_c , N_v , and N_x are the effective densities of states in the conduction, valence, and exciton bands, and $E_x = 14.7 \text{ meV}$ is the binding energy of the exciton ground state. For silicon parameters at $T = 300 \text{ K}$ far away from Mott transition, $n^* = 8 \cdot 10^{17} \text{ cm}^{-3}$.

The second premise was related to the spatial correlation of electron and hole in exciton [14], leading to an essential increase of their Auger recombination probability, in particular, on the impurities. The degree of correlation can be characterized by the effective density of electron-hole pairs in exciton, $n_L = \left(\frac{4}{3}\pi\alpha_B^3\right)^{-1}$, where α_B is the exciton Bohr radius. In silicon, $\alpha_B \approx 4.2$ nm, and $n_L \approx 3.3 \cdot 10^{18}$ cm⁻³. This is a sufficiently high value for the non-radiative Auger recombination to be operative. The inverse lifetime of this process is taken to be

$$\tau_{nr}^{-1} = n_L G N_t, \quad (7)$$

where G is the Auger recombination parameter, and N_t is the density of deep levels.

Let us compare the recombination fluxes due to Shockley–Read–Hall and exciton non-radiative mechanisms, $\Delta n / \tau_{SRH}$ and n_{exc} / τ_{nr} , respectively.

Approximating $\tau_{SRH} \approx (C_t N_t)^{-1}$ and adding these two recombination fluxes by using (6) and (7), we obtain:

$$\frac{\Delta n}{\tau_{SRH}} + \frac{n_{exc}}{\tau_{nr}} \approx \frac{\Delta n}{\tau_{SRH}} \left(1 + \frac{n_0 + \Delta n}{n_x}\right), \quad (8)$$

where $n_x = \frac{n^* G_t}{n_L G}$. (8) has the same form as (1). As for

the difference in the expressions for n_x between this work and [6], it stems from the fact that the latter work neglects the influence of τ_{Auger} on $\tau_{eff}(n)$, while here we take it into account.

The estimates performed in [13] for the case when the deep levels are due to Au impurities give n_x not very different from $8.2 \cdot 10^{15}$ cm⁻³.

Thus, this brief overview of the main results of [13] shows that the experimentally observed dependence $\tau_{eff}(n)$, see (1), can be explained by the non-radiative exciton Auger recombination on the deep impurity levels.

The estimate of the radiative recombination parameter in silicon at $T = 300$ K performed in [10], namely, $A = 6.3 \cdot 10^{-15}$ cm³/s, also took exciton recombination into account. In that work, based on the experimental results from [15] on the temperature dependence of the radiative recombination parameter in silicon, the contributions of the radiative band-to-band and exciton recombination effects could be evaluated separately. It was shown that at room temperature they were comparable [10].

4. Photoconversion efficiency of high-efficiency SCs

Next, we analyze photoconversion efficiency of a SC with the n -type base as a function of the base doping level. In this analysis, we take into account all the recombination mechanisms considered above. The

theoretical results for the efficiency η , open-circuit voltage, V_{OC} , I - V curve fill factor, FF , and some other characteristics are compared to the experimental data. Our analysis employs the semi-empirical model from [16], which allows one to evaluate the performance of a SC based on high-quality crystalline silicon. The feature of this model is that one of the main characteristics, the short-circuit current density, J_{SC} , is taken from the experiment as an input parameter of the theory, from which the remaining characteristics are found theoretically. This considerably simplifies the calculations, which can be used to optimize SCs performance with respect to the base doping level, N_d at given Shockley–Read–Hall lifetime τ_{SRH} , surface recombination velocity on the front and the rear surfaces, S_0 and S_d , and series resistance R_S .

Using the approach from [16], let us write the photoconversion efficiency of the cell characterized by large diffusion lengths, $L_{eff} = \sqrt{D\tau_{eff}} \gg d$, and high excess electron-hole pair density under the open-circuit conditions, $\Delta n_{OC} \geq n_0$. The expression for the open-circuit voltage has the form [17]:

$$V_{OC} \cong \frac{kT}{q} \ln \frac{\Delta n_{OC}}{p_0} + \frac{kT}{q} \ln \left(1 + \frac{\Delta n_{OC}}{n_0}\right), \quad (9)$$

where kT is the thermal energy, q the elementary charge, and $p_0 = n_i^2(T)/n_0$, the equilibrium hole density in the n -type base.

At $\Delta n_{OC} \geq n_0$, the open-circuit voltage is higher than that in the standard case $\Delta n_{OC} < n_0$.

(9) is a quadratic equation for Δn_{OC} , the solution of which is

$$\Delta n_{OC} = -\frac{n_0}{2} + \sqrt{\frac{n_0^2}{4} + n_i^2 \left(e^{qV_{OC}/kT} - 1\right)}. \quad (10)$$

To determine the photoconversion efficiency, we need an expression for the current-voltage curve, which is obtained by replacing V_{OC} in (10) by the applied voltage, V , and including the voltage drop on the series resistance, R_S :

$$\Delta n_{OC} = -\frac{n_0}{2} + \sqrt{\frac{n_0^2}{4} + n_i^2 \left(e^{q(V - J_{SC} R_S)/kT} - 1\right)}, \quad (11)$$

where J is the current density, and A_{SC} – SC area.

The short-circuit current density, J_{SC} , is related to the excess carrier density in the open-circuit regime, Δn_{OC} , by the generation-recombination balance equation. For $L_{eff} \gg d$, it has the form

$$J_{SC} = q \left(\frac{d}{\tau_{eff}} + S \right) \Delta n_{OC}, \quad (12)$$

where $S = S_0 + S_d$ is the net surface recombination velocity on the front and rear surfaces.

Next, we generalize (12) to the case $V < V_{OC}$, when the current through the cell is not non-zero:

$$J(V) = J_{SC} - J_{rec}(V), \quad (13)$$

where the recombination current density is

$$J_{rec}(V) = q \left(\frac{d}{\tau_{eff}} + S \right) \Delta n(V), \quad (14)$$

and τ_{eff} should be found from (2)-(5) with Δn replaced by $\Delta n(V)$.

From the maximum-power condition, $d(VJ(V))/dV = 0$, we can determine V_m , which substitution into (13) allows one to find J_m . As a result, we obtain the maximum photoconversion efficiency and the fill factor:

$$\eta = \frac{J_m V_m}{P_S}, \quad FF = \frac{J_m V_m}{J_{SC} V_{OC}}, \quad (15)$$

where P_S is the power density of incident radiation.

5. Analysis of the exciton non-radiative recombination effect on the SC performance

Shown in Fig. 4 are the theoretical curves for the open-circuit voltage V_{OC} , fill factor FF , and photoconversion efficiency η as a function of the n -type base doping

level. The curves were built using the formulas (12), (10), and (15), with the parameters obtained in the works [2, 18, 19]. The main parameters of these SCs are given in Table I. It was assumed that the surface recombination velocity is independent of the doping level.

In order for non-radiative exciton recombination to have an effect on the photoconversion efficiency of silicon SCs, two conditions must be fulfilled. First, in order for non-radiative recombination to be of comparable rate as the radiative one, we should have $\tau_{SRH} < 20$ ms, as discussed above. This condition is fulfilled for all of the existing p - n junction- and heterojunction-based SCs. The second condition is that the bulk recombination should dominate over the surface recombination. When discussing Fig. 4, we will pay special attention to the latter condition.

As seen in Fig. 4a, the characteristic feature of the $V_{OC}(n_0)$ plot is that, in the low-doping region at large τ_{max} (see (1)), the open-circuit voltage decreases with the dopant density. However, as τ_{max} is reduced, these curves begin to grow. At the same time, FF and η increase with the doping level even at the largest efficiency value of about 25%. Non-radiative exciton recombination leads to a decrease of V_{OC} , FF , and η , which depends on the doping level, τ_{SRH} , and S . As seen in Fig. 4c, at the

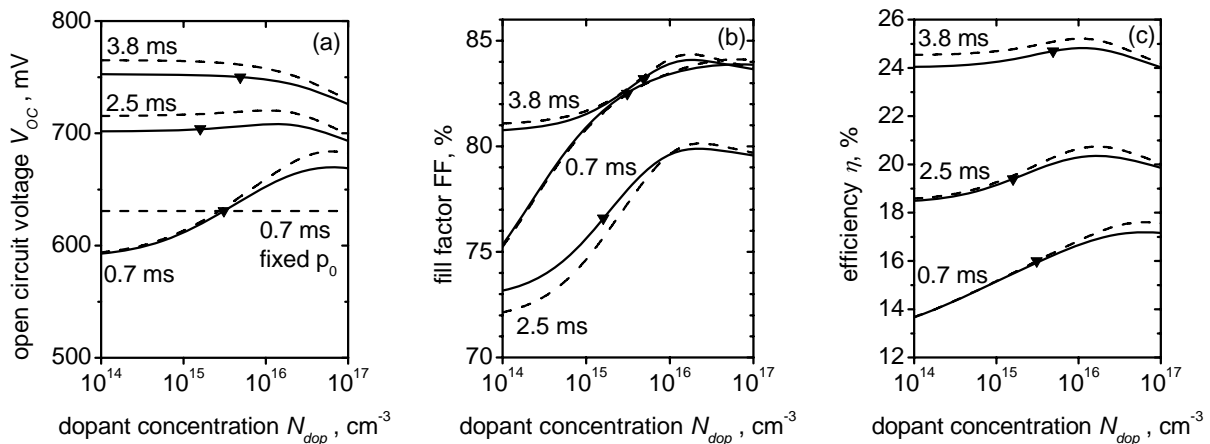


Fig. 4. Open-circuit voltage, I - V curve fill factor, and photoconversion efficiency vs. the doping level obtained with (solid lines) and without (dashed lines) taking exciton recombination into account for different values of τ_{SRH} . The symbols are the experimental points, as indicated in Table I.

Table. Parameters from Refs. [2, 18, 19] and obtained using Eqs. (9)-(15).

Ref.	N_{d_3} , cm ⁻³	d , μ m	τ_{max} , ms	J , mA/cm ²	V_{OC} , mV	FF , %	η , %	S , cm/s	A_{SC_2} , cm ²	R_S , Ohm
[2]	$4.9 \cdot 10^{15}$	98	3.8	39.5	750	83.2	24.7	1.5	100	0.0027
[18]	$1.6 \cdot 10^{15}$	300	2.5	36	704	76.6	19.4	12	4	0.25
[19]	$3.1 \cdot 10^{15}$	380	0.7	30.6	631	82.5	16.0	220	2	0.03

minimal surface recombination velocities and $\tau_{SRH} \approx 4$ ms, the difference between the theoretical efficiency with and without exciton recombination taken into account for the upper two curves is slightly reduced with increasing n_0 and is only 1.5%. For $S = 12$ cm/s and $\tau_{SRH} \approx 2.5$ ms (see these two middle curves), the difference increases from less than 1% at $N_d \approx 10^{15}$ cm $^{-3}$ to 2% at the doping level corresponding to the maximal efficiency, *i.e.*, $n_0 = 2 \cdot 10^{16}$ cm $^{-3}$. Finally, at $S = 220$ cm/s and $\tau_{SRH} \approx 0.4$ ms (the lowest two curves), the difference between the theoretical efficiencies obtained with and without exciton recombination increases from less than 1% at $N_d \approx 10^{15}$ cm $^{-3}$ to 2% at $N_d \approx 6 \cdot 10^{16}$ cm $^{-3}$ corresponding to the highest efficiency.

According to the parameters from Table I, for these two upper curves, the bulk recombination velocity $V_b = d/\tau_{eff}$ is 2.6 cm/s at low doping levels, and the surface recombination velocity is 1.5 cm/s, *i.e.*, the second condition for the non-radiative exciton recombination to manifest itself is fulfilled. This is not the case for the other two pairs of curves, for which $V_b = S = 12$ cm/s (middle curve) and $V_b = 54$ cm/s, $S = 220$ cm/s (lower curve), for which surface recombination dominates.

Thus, for the parameters from Table I, the largest effect of exciton recombination on the main SC characteristics is about 2%.

Fig. 5 shows the photoconversion efficiency on the Shockley–Read–Hall lifetime dependence, plotted for the parameters from the third row of Table I for $n_0 = 2 \cdot 10^{16}$ cm $^{-3}$. In this case, the efficiency is maximal or close to its maximum. For these three pairs of curves, we took $S = 1.5$ cm/s (two upper curves), $S = 12$ cm/s (middle curves), and $S = 220$ cm/s (lower curves). As seen from the figure, the smaller τ_{SRH} , the larger the efficiency decrease due to the non-radiative exciton recombination. The largest difference between the curves obtained with and without its effect taken into account is observed at the smallest Shockley–Read–Hall lifetime $\tau_{SRH} = 100$ μ s and is about 5.5%.

We note that upon further decrease of the Shockley–Read–Hall lifetime from 100 to 1 μ s, exciton recombination leads to the reduction of photoconversion efficiency, which is the stronger the smaller τ_{SRH} . For instance, at $\tau_{SRH} \approx 1$ μ s, this reduction reaches $\approx 25\%$ for *n*-type base and $\approx 45\%$ for *p*-type base.

In the work [20], the influence of various excitonic effects on the photoconversion in silicon structures with *p-n* junctions, including the non-radiative recombination, was analyzed. However, in determination of n_x , when comparing the theoretical and experimental $\tau_{eff}^{-1}(n_0)$ curves, the radiative recombination rate was underestimated, and band-to-band Auger recombination was not taken into account. This resulted in an overestimation of n_x that was found to be $3.7 \cdot 10^{15}$ cm $^{-3}$.

In the work [19], τ_{Auger} was evaluated using the empirical formulas from [13] and [21] as well as the experimental dependence of the Auger recombination lifetime on the doping level n_0 , which were different

from those in [5]. Namely, within the range $10^{15} < n_0 < 10^{16}$ cm $^{-3}$, the results for $\tau_{Auger}(n_0)$ in [5] and [16] are quite close, but for $n_0 > 10^{16}$ cm $^{-3}$ a discrepancy exists between these two sets of data, with $\tau_{Auger}(n_0)$ decreasing with n_0 more slowly in [16] than in [5]. As a result, calculations of the efficiency η vs. the doping level n_0 based on $\tau_{Auger}(n_0)$ curve from [16] yield a maximum efficiency at a larger value of n_0 , with a somewhat higher peak efficiency. However, the conclusion about the necessity of a heavier base doping than in [2, 18, 19] to increase the SC efficiency remains valid. Moreover, as calculations show, the photoconversion efficiency at the experimentally used doping levels, obtained for different expressions of $\tau_{Auger}(n_0)$, differ by more than 2%.

As shown in [20], calculation of the open-circuit voltage, V_{OC} , and photogenerated voltage in the maximum-power regime, V_m , should be done taking into account the thermodynamic effect of the excitons discussed in [22-24]. This effect has to do with the reduction of the excess electron-hole pair density in the maximal-power regime, n_m , due to the binding of some electrons and holes into excitons, leading to the reduction of V_{OC} and V_m . For the case considered here, $\Delta n_m \geq n_0$, the following relation holds:

$$V_m \approx V_m^* - \frac{2kT}{q} \ln \left(1 + \frac{n_0 + \Delta n_m}{n^*} \right) + \frac{kT}{q} \ln \left(1 + \frac{n_0}{n^*} \right), \quad (16)$$

where V_m^* is the photogenerated voltage in the maximum-power regime without taking the thermodynamic effect of exciton into account.

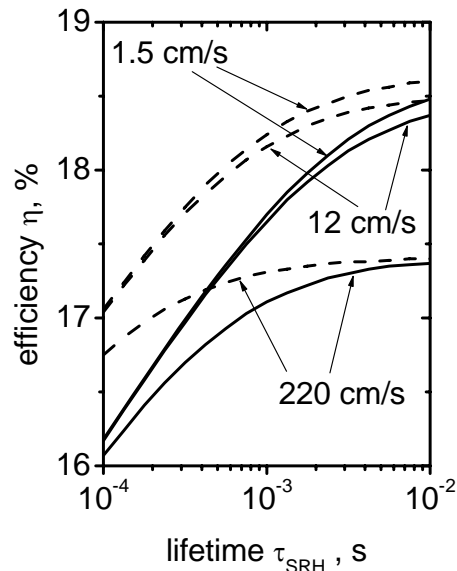


Fig. 5. Photoconversion efficiency vs. the Shockley–Read–Hall lifetime for SC parameters from Ref. [19] for different values of surface recombination velocity. Solid lines are obtained taking into account exciton recombination, and dashed lines are obtained without accounting for this effect.

Estimates based on the parameter values, at which V_{OC} and V_m are maximized, show that the ratio of the difference between the latter two terms in (16), which take the exciton effect into account, to V_m does not exceed 0.5% at $n_0 = 10^{17} \text{ cm}^{-3}$, and is about 0.03% at $n_0 = 5 \cdot 10^{15} \text{ cm}^{-3}$. This allows us to neglect the thermodynamic exciton effect.

We note that in [24], a recombination contribution of the form (1) was used in the expression for the effective lifetime in silicon, but was not connected to the non-radiative exciton recombination.

In high-efficiency heterojunction silicon SCs, exciton radiative recombination is negligible. According to [9], the radiative exciton recombination parameter in silicon is $2.6 \cdot 10^{15} \text{ cm}^3/\text{s}$, whereas the ratio of the radiative to non-radiative exciton recombination rates at $n_0 = 5 \cdot 10^{15} \text{ cm}^{-3}$ and $\tau_{SRH} \approx 4 \text{ ms}$ is $4 \cdot 10^{-4}$. Thus, out of three exciton effects – the thermodynamic effect, radiative and non-radiative recombination – it is the non-radiative Auger recombination on deep impurity levels that is the strongest.

Finally, let us sum up the criteria that allow one to describe the influence of non-radiative exciton recombination on the photoconversion efficiency in silicon SCs.

6. Conclusions

As the analysis of the dependence of experimental bulk lifetime in silicon on the doping and excitation levels has shown, at $\tau_{SRH} < 20 \text{ ms}$, an additional recombination channel related to non-radiative exciton recombination starts to manifest itself. The smaller τ_{SRH} , the stronger its contribution. The nature of the bulk lifetime reduction in silicon at the doping or excitation level of about 10^{16} cm^{-3} was shown to be unrelated to technological factors, but is due to the non-radiative exciton recombination on the deep levels.

Taking this channel into account does not change the conclusions of [16] regarding the optimization of the doping level. As seen in Figs. 4b and 4c, the optimal doping level related to the comparable contributions from Shockley–Read–Hall recombination and band-to-band Auger recombination is about $2 \cdot 10^{16} \text{ cm}^{-3}$ at the minimized surface recombination velocity S and increases to about 10^{17} cm^{-3} with S .

References

1. M.A. Green, The path to 25% silicon solar cell efficiency: History of silicon cell evolution // *Prog. Photovolt: Res. Appl.* **17**, p. 183-189 (2009).
2. K. Masuko, M. Shigematsu, T. Hashiguchi et al., Achievement of more than 25% conversion efficiency with crystalline silicon heterojunction solar cells // *IEEE J. Photovolt.* **4**(6), p. 1433-1435 (2014).
3. A. Jano, S. Tohoda, K. Matsuyama, Y. Nakamura, T. Nishiwaki, K. Fujita, M. Taguchi, and E. Maruyama, 24.7 record efficiency hit solar cell on thin silicon wafer // *Proc. 28-th European Photovoltaic Solar Energy Conference and Exhibition*, Paris, France, 2013, p. 1846-1848.
4. E. Yablonovitch and T. Gmitter, Auger recombination in silicon at low carrier densities // *Appl. Phys. Lett.* **49**(10), p. 587-589 (1986).
5. A. Richter, S. Glunz, F. Werner, J. Schmidt et al., Improved quantitative description of Auger recombination in crystalline silicon // *Phys. Rev.* **86**, 165202 (2012).
6. J.G. Fossum, Computer-aided numerical analysis of silicon solar cells // *Solid State Electron.* **19**(4), p. 269-277 (1976).
7. D. Kendall, *Proc. Conference for Physics and Application of Lithium Diffused Silicon*, NASA Space Flight Center, Goddard, FL (1969).
8. K. Gra, H. Pieper and G. Goldbach, *Semiconductor Silicon*. 1973.
9. R. Häcker, A. Hangleiter, Intrinsic upper limits of the carrier lifetime in silicon // *J. Appl. Phys.* **75**(11), p.7570-7572 (1994).
10. A.V. Sachenko, A.P. Gorban, V.P. Kostilyov, I.O. Sokolovsky, The radiative recombination coefficient and the internal quantum yield of electroluminescence in silicon // *Semiconductors*, **40**(8), p. 884-889 (2006).
11. J.D. Beck, R. Conradt, Auger-recombination in Si // *Solid State Commun.* **13**, p. 93-95 (1973).
12. L. Passari, E. Susi, Recombination mechanisms and doping density in silicon // *J. Appl. Phys.* **54**, p. 3935-3937 (1983).
13. A.V. Sachenko, A.P. Gorban, V.P. Kostilyov, Exciton-enhanced recombination in silicon at high concentrations of charge carriers // *Semiconductor Physics, Quantum Electronics & Optoelectronics*, **3**, p. 5-10 (2000).
14. A. Hangleiter, Nonradiative recombination via deep impurity levels in silicon: Experiment // *Phys. Rev. B*, **35**(17), p. 9149-9160 (1987); A. Hangleiter, Nonradiative recombination via deep impurity levels in semiconductors: The exciton Auger mechanism // *Phys. Rev. B*, **37**(5), p. 2594-2604 (1988).
15. T. Trupke, M.A. Green, P. Würfel, P.P. Altermatt et al., Temperature dependence of the radiative recombination coefficient of intrinsic crystalline silicon // *J. Appl. Phys.* **94**(8), p. 4930-4937 (2003).
16. A.V. Sachenko, A.I. Shkrebti, R.M. Korkishko, V.P. Kostilyov et al., Features of photoconversion in highly efficient silicon solar cells // *Semiconductors*, **49**(2), p. 264-269 (2015).
17. A.P. Gorban', A.V. Sachenko, V.P. Kostilyov, N.A. Prima, Effect of excitons on photoconversion efficiency in the p^+n-n^+ and n^+p-p^+ -structures based on single-crystalline silicon // *Semiconductor*

- Physics, Quantum Electronics & Optoelectronics*, **3**(3) p. 322-329 (2000).
18. R. Gogolin, R. Ferre, M. Turcu, N.-P. Harder, Silicon heterojunction solar cells: Influence of H₂-dilution on cell performance // *Solar Energy Materials & Solar Cells*, **106**, p. 47-50 (2012).
 19. A.V. Sachenko, V.P. Kostylyov, R.M. Korkishko, M.R. Kulish, V.M. Vlasiuk, D.V. Khomenko, Peculiarities of the temperature dependences of silicon solar cells illuminated with light simulator // *Semiconductor Physics, Quantum Electronics & Optoelectronics*, **18**(3), p. 259-266 (2015).
 20. A.V. Sachenko, N.A. Prima, A.P. Gorban, A.A. Serba, Effect of excitons on the upper limit of conversion efficiency in silicon solar cells // *Proc. 17-th European Photovoltaic Solar Energy Conference*, Munich, Germany, 2001, p. 230-233.
 21. A.V. Sachenko, A.P. Gorban, V.P. Kostylyov, I.O. Sokolovskyi, The square law recombination in silicon and its effect as far as the volume life time is concerned // *Semiconductors*, **41**(3), p. 290-294 (2007).
 22. D.E. Kane, R.M. Swanson, The effect of excitons on apparent band gap narrowing and transport in semiconductors // *J. Appl. Phys.* **73**(3), p. 1193-1197 (1993).
 23. R. Corkish, S.-P. Chan, M.A. Green, Excitons in silicon diodes and solar cells: A three-particle theory // *J. Appl. Phys.* **79**(1), p. 195-203 (1993).
 24. M.A. Green, Excitons in silicon solar cells: room temperature distributions and flows // *Proc. Photovoltaic Solar Energy Conversion Conference*, Vienna, 1998, p. 74-76.